Modeling Detonation Propagation and Failure Using Explosive Initiation Models in a Conventional Hydrocode

John Starkenberg
U.S. Army Research Laboratory
Aberdeen Proving Ground, Maryland

Explosive shock initiation models are sometimes used to predict detonation propagation and failure behavior. A detailed examination of the representation of detonation achieved using CTH and its History Variable Reactive Burn (HVRB) and Ignition and Growth reaction rate models was made. Both planar and curved detonation propagation were considered. Ignition and Growth was deemed unsuitable for detonation modeling because of the difficulty involved in calibrating its fifteen constants. Although full advantage has not yet been taken of its capability to represent burning topology, HVRB is a more suitable candidate. Existing HVRB calibrations with pressure exponents of 4.0 produced unsteady planar detonations. Existing Ignition and Growth calibrations concentrated too much reaction in the shock and showed significant discontinuities in the slope of the reaction variable profile as control shifted from one term to another. Simple modifications of existing HVRB calibrations were sufficient to produce reasonably accurate representations of the effect of charge diameter on detonation velocity.

Background

A number of reaction rate models for explosive shock initiation have been developed and used in hydrocode simulations to predict results from a variety of experiments. The results are sometimes quite accurate (Starkenberg 1989), requiring only moderate computational resolution to capture the initiation process. For some classes of problems they are notoriously inaccurate. These models are commonly calibrated with reference to wedge test data giving the time and distance of run to detonation as a function of initial shock pressure (Pop plots). They grossly simplify details of the physical processes involved. As a result, it may not be possible to model the response of an energetic material over a wide range of pressures with the same calibration.

Initiation models are sometimes used to predict detonation propagation and failure behavior. In this case, resolution requirements are more stringent, and problems with convergence of solutions have sometimes been observed, especially when modeling detonation failure. Although Detonation Shock Dynamics (Bdzil 1989; Aslam, Bdzil, and Hill 1998) was developed for modeling curved detonation propagation, the allowable forms of the reaction rate law are re-

stricted and unsteady flows (such as those associated with detonation failure) are precluded. It has not yet been shown to produce accurate predictions of "rate-stick" experiments, and has not been made available in widely distributed continuum mechanics software. Use of a reaction rate model in a conventional hydrocode is a more generally available option. Menikoff, Lackner, and Bukiet (1996) have shown that the details of the reaction rate model do not strongly influence curved detonation propagation behavior. This gives some cause to hope that, with appropriate calibrations, the reaction rate models can provide an adequate representation of detonation propagation even though the details of these models are likely to be incorrect.

In order to gain a clearer understanding of the requirements for simulating detonation using these models, a detailed examination of the representation of detonation achieved using CTH and its History Variable Reactive Burn (HVRB) and Ignition and Growth rate models was made. Both planar and curved detonation propagation were considered. Accurate modeling requires adequate resolution of the reaction zone, including isolation of the reaction rate process from shock compression captured using artificial viscosity (wherein time scales are distorted). A range of computational zone sizes was considered. Materials modeled include Composition B3, Octol, and LX-17 among others.

CTH

CTH (Hertel et al. 1993) provides capabilities for modeling dynamics of multidimensional systems with multiple materials, large deformations, and strong shock waves. It is described as an ongoing project of the Sandia National Laboratories. It includes up-to-date material models and up-to-date material models and incorporates the History Variable Reactive Burn (Kerley 1992; Starkenberg 1998), Forest Fire (Mader 1970; Mader 1979; Lundstrom 1988; Starkenberg 1993), and Ignition and Growth (Lee and Tarver 1980) explosive initiation models.

Reaction Rate Models

Reaction rate models for explosive initiation can be broadly categorized as single-step or multiple-step. The former category is characterized by a single rate equation describing the progress of a single reaction variable, usually the reacted mass fraction. Examples in this category include Forest Fire, Ignition and Growth and HVRB. The latter category is characterized by two or more linked rate models for two or more reaction variables. The most primitive of these variables often represents the hot-spot population. This category is exemplified by the Johnson-Tang-Forest (JTF 1985) model.

General Forms. Although chemical reaction rates are properly represented as temperature dependent, reaction rate models used for explosive burn in hydrocodes are usually pressure dependent. The general form taken by many of the single-step models consists of a series of terms, each including a mass-fraction-dependent function representing burning topology and a pressure-dependent function representing the burn rate.

$$\dot{\lambda} = \sum_j s_j(\lambda) \cdot r_j(p,\rho,\cdots).$$

Common burning topologies include bulk reaction,

$$s(\lambda) \sim (1-\lambda),$$

hole-burning surface reaction,

$$s(\lambda) \sim \lambda^{2/3},$$

and grain-burning surface reaction,

$$s(\lambda) \sim (1-\lambda)^{2/3}.$$

The surface reaction functions are applicable to surfaces that remain geometrically self-similar under uniform regression. Clearly, this condition does not generally prevail. This is most commonly accounted for by modifying the exponents. Thus, generalized hole burning is given by

$$s_h(\lambda) \sim \lambda^{n_h}.$$

This dependence causes the reaction rate to vanish initially and increase as reaction proceeds. Generalized grain burning is given by

$$s_g(\lambda) \sim (1-\lambda)^{n_g}.$$

This produces a maximum initial rate, which decreases as reaction proceeds. These topology functions are combined to produce the generalized topology function,

$$s(\lambda) = s_h(\lambda) \cdot s_g(\lambda),$$

which vanishes at the beginning and end of reaction with a maximum somewhere between. Evidence suggests that, while the hole-burning assumption may be appropriate at the beginning of reaction, grain burning is often the dominant process. Other factors may play important roles. However, the present work addresses only the performance of the models in representing detonation. In this regard, it is encouraging that propagation of curved detonations has been shown to be sensitive only to gross features and not to details of the reaction rate model used.

Ignition and Growth. The reaction rate expression for the Ignition and Growth model, as implemented in CTH, is given by

$$\begin{aligned}
\dot{\lambda} = {} & g_0 \cdot (1-\lambda)^{n_1} \cdot (\rho/\rho_0 - 1 - a_0)^{n_\rho} && \lambda < \lambda_0 \\
& + g_1 \cdot (1-\lambda)^{n_{g1}} \cdot \lambda^{n_{h1}} \cdot p^{n_{p1}} && \lambda < \lambda_1 \\
& + g_2 \cdot (1-\lambda)^{n_{g2}} \cdot \lambda^{n_{h2}} \cdot p^{n_{p2}} && \lambda > \lambda_2 .
\end{aligned}$$

This model consists of an "ignition" and two "growth" terms. The ignition term is density rather than pressure dependent and includes a compression threshold, a_0, for reaction onset. It has a burning topology represented by grain burning, even though hole burning is more applicable at the beginning of reaction. The growth terms are consistent with the generalized form given previously, incorporating representations of both hole and grain burning. Although this is a single-step model, its terms are used to mimic the behavior of a multiple-step model, by turning them on and off at specified values of the mass fraction. This model requires the calibration of fifteen constants and is probably more detailed than is required for the representation of detonation propagation and failure. Typical values of the Ignition and Growth calibration exponents found in the CTH library (Kerley 1992) are given in Table 1. The facts that the ignition topology corresponds to grain burning and the ignition density exponent is given the astronomical value of 20 indicate that this term is an artifice to initiate reaction at lower shock pressures. In some cases self-similar hole and grain burning is specified for the first growth term (n_{g1}=⅔). The second growth term is often given a topology consistent with bulk reaction (n_{g2}=1). In general, however, topology exponents are manipulated to

Table 1. Typical values of Ignition and Growth exponent calibration constants.

		Hole Burning	Grain Burning	Density/Pressure
Ignition Term		n/a	2/9, 2/3	20
Growth Terms	1st	1/9, 2/3	1/9, 2/9, 2/3	1, 1.4
	2nd	1	1/3, 1	2, 3

fix the value of the reaction variable for which the topology function is maximized or to fit gauge data when available. The pressure exponents of the two growth terms do not generally exceed a value of 3.0 and are often lower.

HVRB. HVRB is formulated in a somewhat different manner. A "history variable" ϕ is defined as a function of pressure:

$$\varphi = \int_0^t \left(\frac{p - p_i}{p_s} \right)^{n_p} \frac{d\tau}{\tau_s},$$

where p_s and τ_s are scaling constants that represent only one independent calibration constant. The reaction variable is then related to the history variable:

$$\lambda = 1 - \left(1 - \frac{\varphi^{n_\varphi}}{n_\lambda} \right)^{n_\lambda}.$$

This model has only five calibration constants, and is probably adequate for representation of detonation propagation and failure. However, it is not given in a form consistent with the generalized rate model. This can be corrected by differentiating:

$$\dot{\lambda} = n_\varphi \cdot n_\lambda^{1-1/n_\varphi} \cdot (1-\lambda)^{1-1/n_\lambda} \cdot [1-(1-\lambda)^{1/n_\lambda}]^{1-1/n_\varphi} \cdot \dot{\varphi},$$

where

$$\dot{\phi} = \frac{1}{\tau_s} \left(\frac{p - p_i}{p_s} \right)^{n_p}.$$

The associated burning topoplogy can be elucidated by defining

$$n_h = 1 - 1/n_\phi,$$

and

$$n_g = 1 - 1/n_\lambda.$$

This gives

$$\dot{\lambda} = k_s \cdot (1-\lambda)^{n_g} \cdot [1-(1-\lambda)^{1-n_g}]^{n_h} \cdot (p - p_i)^{n_p}$$

with

$$k_s = [(1-n_h) \cdot (1-n_g)^{n_h} \cdot \tau_s \cdot p_s^{n_p}]^{-1}.$$

The burning topology function, then, is given by

$$s(\lambda) = (1-\lambda)^{n_g} \cdot [1-(1-\lambda)^{1-n_g}]^{n_h},$$

and the hole- and grain-burning topology functions can be identified as

$$s_h(\lambda) = [1-(1-\lambda)^{1-n_g}]^{n_h},$$

and

$$s_g(\lambda) = (1-\lambda)^{n_g}.$$

The HVRB hole-burning topology function differs somewhat from the conventional form in that it depends on both the hole-burning and grain-burning exponents. However, pure hole burning is obtained with $n_g = 0$ (n_λ=1) and pure grain burning with $n_h = 0$ (n_ϕ=1). All HVRB calibrations found in the CTH library are consistent with pure hole burning throughout the reaction process! This means that the reaction rate is maximized as the unreacted material is depleted. This is not a very realistic representation. The hole-burning exponent varies between 0.09 and 0.75. The pressure exponent varies between 2.3 and 5.7! Thus, some very strong pressure dependencies are found. Typical burning topology functions are plotted in Figure 1. These include pure hole burning, pure grain burning, and combined hole and grain burning (maximum at $\lambda = 0.5$). In spite of the difference in the hole-burning topology function, these show the expected features.

Simulating Detonation

For a hydrocode simulation to properly represent detonation at least two conditions must be met: 1) the reaction zone must be sufficiently resolved, and 2) the reaction zone must be adequately isolated from the leading shock compression. The latter con-

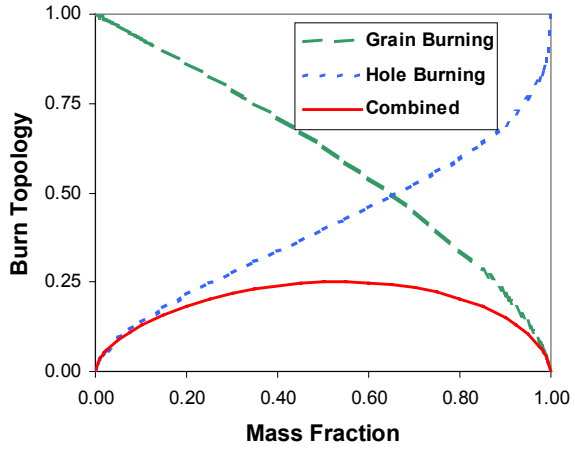

Figure 1. Typical burning topology functions.

dition is required because the shock rise time is governed by artificial viscosity, is dependent on zone size, and is much longer than the physical rise time of the shock. The condition is not explicitly enforced in CTH but, as a practical matter, this condition is met with sufficient accuracy when the reaction-zone resolution is high enough and/or the reaction rate is low enough.

Two propagation modes are considered here. In both cases, a programmed-burn segment was used to initiate the charge. The simplest of these is planar detonation in charges of infinite lateral dimensions. In this case, the detonation remains planar but may be steady or unsteady. These problems can be simulated on relatively small computational grids, even with fine zoning. They were represented using a two-dimensional rectangular mesh consisting of uniform square zones (50 in the lateral direction and 500 in the direction of propagation.

Curved detonation in cylindrical charges was also simulated. In this case, consideration is limited to steady detonation, the detonation velocity is a function of charge radius and detonations fail to propagate when the radius is too small. These problems require much larger computational grids. They were represented using a two-dimensional cylindrical mesh consisting of uniform square zones. As many as 10 million zones were required in some simulations.

The effects of parameters representing the pressure dependence are considered here. The effects of topology parameters have not yet been addressed.

Planar Detonation: Steady and Unsteady. Planar detonation in an infinite charge was simulated using the CTH library HVRB calibration for LX-17. This calibration has a pressure exponent of 4.0. The simulation was performed in a two-dimensional rectangular mesh with 0.01-mm square zones. Reflecting lateral boundaries are used to represent an infinite charge. The detonation remains planar. Profile plots of pressure and reaction variable at various times are shown in Figure 2. These indicate a strong periodic unsteadiness. The abrupt change in slope of the reaction variable at the end of reaction is an artifact of the hole-burning representation. Along with results obtained in simulations with coarser zones, these show that the average period and minimum and maximum reaction zone thickness are converged. This observation is summarized in Table 2.

Table 2. Convergence of unsteady detonation in an infinite LX-17 charge.

Zone Size (mm)	Period (μs)	Reaction Zone Thickness			
		minimum		maximum	
		mm	zones	mm	zones
0.020	0.26	0.10	5	0.42	21
0.010	0.23	0.08	8	0.39	39
0.005	0.23	0.08	16	0.37	74

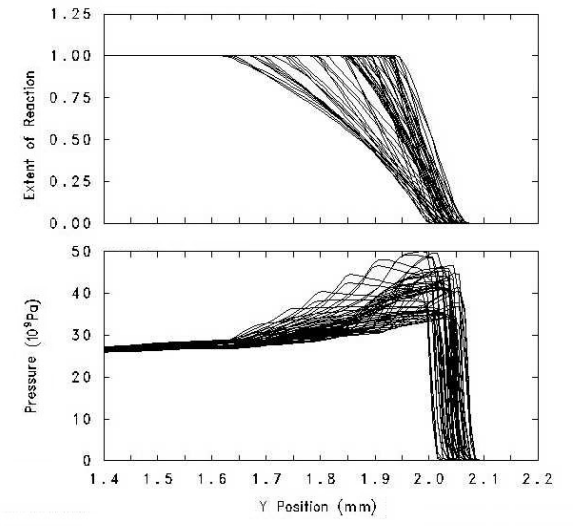

Figure 2. Pressure and reaction variable profiles every 0.02 μs over the period of 1.0 μs showing periodic unsteadiness in an LX-17 detonation using HVRB.

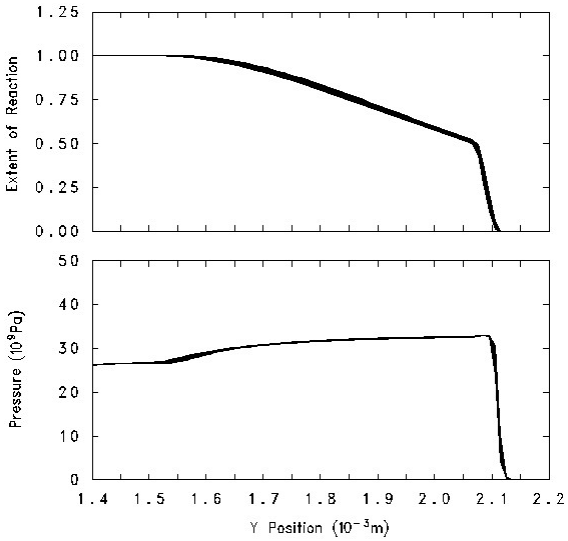

Figure 3. Pressure and reaction variable profiles every 0.02 μs over the period of 1.0 μs showing steady detonation of an LX-17 charge using Ignition & Growth.

A similar simulation was performed with the CTH library Ignition-and-Growth calibration for LX-17. The pressure exponents in this calibration do not exceed 3.0. The pressure and reaction variable profiles, shown in Figure 3, overlay one another nearly exactly, indicating steady detonation. The slope of the reaction variable profile changes at 50% reaction. This is where the ignition and first growth term are turned off. Most of the reaction zone is represented by the second growth term for which the pressure exponent is 3.0. About a quarter of the reaction occurs during the shock compression. This part is governed by the ignition and first growth terms. The very high ignition compression exponent is intended for use at lower initiation pressures. It causes undesirable significant immediate reaction at detonation pressure levels.

Further simulations were performed with a variety of CTH library HVRB calibrations representing a number of materials. The results are summarized in Table 3. Unsteady planar detonations were observed for three calibrations with a pressure exponent of 4.0. The result for nitromethane with a higher pressure exponent is steady. In this case, the hole-burning exponent is much higher than the prevailing value for the unsteady cases. The relative importance of these two parameters in producing unsteadiness is not clear. Equation of state parameters may also influence the results. The scaling pressure, p_s, can also affect the steadiness of a detonation. Results for Octol with several different scaling pressures are shown in Table 4. Unsteadiness increases with scaling pressure.

Table 3. Detonation steadiness for a number of CTH library HVRB calibrations in order of increasing pressure exponent.

Explosive	Pressure Exponent	Hole-Burning Exponent	Planar Detonation
Octol	2.70	0.3333	steady
PETN	2.97	0.2308	steady
Compositon B3	3.00	0.3333	steady
EL-506A	3.50	0.3333	steady
EL-506B	3.50	0.3333	steady
XTX-8003	3.50	0.3333	steady
TNT	3.80	0.3333	steady
Composition C4	3.80	0.3333	steady
LX-17	4.00	0.0909	unsteady
PBX-9502	4.00	0.0909	unsteady
TATB	4.00	0.0909	unsteady
Nitromethane	5.70	0.7500	steady

Table 4. Detonation steadiness in Octol at different values of the scaling pressure.

Scaling Pressure (GPa)	Planar Detonation
7.5	steady
8.0	steady
9.0	steady
10.0	<unsteady
11.0	>unsteady
12.0	unsteady

Curved Detonation in Cylindrical Charges. Simulations using the CTH library HVRB calibration for Composition B3 were performed using square 0.02-mm zones. The detonation velocity normalized with respect to the infinite charge value is plotted as a function of propagation distance in charge diameters in Figure 4. The programmed burn is amplified to ensure that the detonations start out overdriven. The results show that the curved detonation is also steady until the charge radius approaches the failure radius. The wave for the 6.0-mm-diameter charge may be slowly failing.

Detonation propagation experiments that give the detonation velocity as a function of charge radius (Campbell and Engelke 1976) can be used to evaluate the accuracy of the initiation models in representing curved detonation propagation. Not surprisingly, it was necessary to recalibrate HVRB to obtain an accurate representation of these experiments. In the case of Octol, the library Popplot calibration produces detonation velocities that are too high. This is shown in Figure 5. Using the CTH library calibration, the detonation velocity as a function of charge diameter was determined at zone sizes of 0.04, 0.02, and 0.01 mm. There is evidence of convergence at the two finer zone sizes. Much closer agreement between

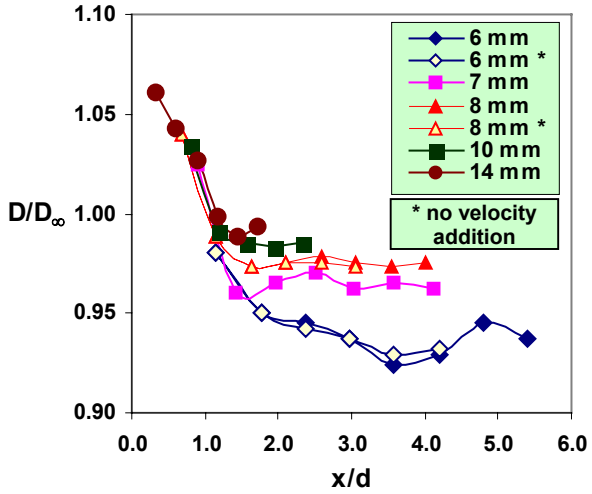

Figure 4. Normalized detonation velocity as a function of propagation distance in diameters in Composition B3 charges at various diameters.

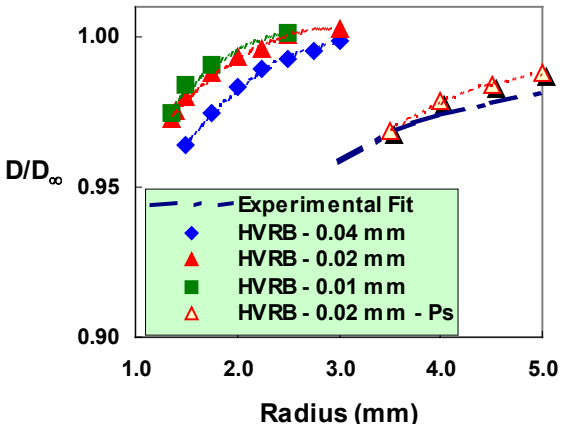

Figure 5. HVRB predictions of normalized detonation velocity for Octol as a function of charge radius for several computational zone sizes compared with a fit to experimental data.

the CTH/HVRB predictions and the experimental results is achieved by simply increasing the scaling pressure from 7.5 GPa to 11.3 GPa.

Several issues remain to be explored. Convergence of solutions for the failure diameter has not been established. The Grüneisen coefficient associated with the unreacted explosive equation of state is not

well known. Its effect on detonation propagation and failure has not been explored.

Summary and Conclusions

Ignition and Growth was deemed unsuitable for detonation modeling because of the difficulty involved in calibrating its fifteen constants. Although full advantage has not yet been taken of its capability to represent burning topology, HVRB is a more suitable candidate.

Existing HVRB calibrations with high pressure and hole-burning exponents produce unsteady planar detonations. Existing Ignition and Growth calibrations concentrate too much reaction in the shock and show significant discontinuities in the slope of the reaction variable profile as control shifts from one term to another.

Because Ignition and Growth was deemed inappropriate, modeling of curved detonation propagation was pursued with HVRB only. Results achieved with waves that are stationary in the computational mesh compare favorably with those for waves that propagate through the mesh. HVRB is suitable for modeling detonation. However, the calibrations obtained using initiation data are not accurate for detonation. Simple modifications of existing calibrations were sufficient to produce reasonably accurate representations of the effect of charge diameter on detonation velocity.

References

Aslam, T. D., J. B. Bdzil, and L. G. Hill. "Extensions to DSD Theory: Analysis of PBX 9502 Rate Stick Data." *Proceedings of the Eleventh International Detonation Symposium,* pp. 21–29, Snowmass, CO, August 1998.

Bdzil, J. B., W. Fickett, and D. S. Stewart. "Detonation Shock Dynamics: A New Approach to Modeling Multi-Dimensional Detonation Waves." *Proceedings of the Ninth Symposium (International) on Detonation,* pp. 730–742, Portland, OR, August 1989.

Campbell, A. W., and R. Engelke. "The Diameter Effect in High-Density Heterogeneous Explosives." *Proceedings of the Sixth Symposium (International) on Detonation,* pp. 642–652, Coronado, CA, August 1976.

Hertel, E. S. Jr., R. L. Bell, M. G. Elrick, A. V. Farnsworth, G. I. Kerley, J. M. McGlaun, S. V. Petney, S. A. Silling, P. A. Taylor and, L. Yarrington. "CTH: A Software Family for Multi-Dimensional Shock Physics Analysis." *Proceedings of the 19th International Symposium on Shock Waves,* vol. 1, pp. 377–382, July 1993.

Johnson, J. N., P. K. Tang, and C. A. Forest. "Shock Wave Initiation of Heterogeneous Reactive Solids." *Journal of Applied Physics,* vol. 57, no. 9, 1985.

Kerley, G. I. "CTH Equation of State Package: Porosity and Reactive Burn Models." SAND92-0553, Sandia National Laboratories, NM, April 1992.

Lee, E. L., and C. M. Tarver. "Phenomenological Model of Shock Initiation in Heterogeneous Explosives." *Physics of Fluids,* vol. 23, no. 12, pp. 2362–2372, December 1980.

Lundstrom, E. A. "Evaluation of Forest Fire Burn Model of Reaction Kinetics of Heterogeneous Explosives." Naval Weapons Center Technical Publication 6898, Naval Weapons Center, CA, 1988.

Mader, C. L. “An Empirical Model of Heterogeneous Shock Initiation of 9404.” Report LA-4475, Los Alamos Scientific Laboratory, Los Alamos, NM, 1970.

Mader, C. L. *Numerical Modeling of Detonation***.** University of California Press, Berkeley, 1979.

Mader, C. L., and C. A. Forest. “Two Dimensional Homogeneous and Heterogeneous Detonation Wave Propagation.” Report LA-6259, Los Alamos Scientific Laboratory, Los Alamos, NM, 1976.

Menikoff, R, K. S. Lackner, and B. G. Bukiet. “Modeling Flows with Curved Detonation Waves.” *Combustion and Flame*, 104, pp 219–240, 1996.

Starkenberg, J. “A Model for the Initiation of Heterogeneous High Explosives Subject to General Compressive Loading.” *Proceedings of the Ninth Symposium (International) on Detonation,* pp. 604–617, Portland, OR, August 1989.

Starkenberg, J. “An Assessment of the Performance of the Original and Modified Versions of the Forest Fire Explosive Initiation Model.” *Proceedings of the Tenth International Detonation Symposium,* pp. 992–1002, Boston, MA, July 1993.

Starkenberg, J. “An Assessment of the Performance of the History Variable Reactive Burn Explosive Initiation Model in the CTH Code.” *Proceedings of the Eleventh International Detonation Symposium,* p. 621–631, Snowmass, CO, September 1998.